Computer Fraud and Security
ISSN (online): 1873-7056

Adaptive Threshold Cloud Detection Method based on Gaofen-1 Remote Sensing image

Wenfa Xu[1], Qing Li[1*], Shumin Fan[2], Shiqiang Wen[3,4,5], Mingzhi Xiao[1], Xiong Yang[6]

[1]School of Information Science and Engineering, Wuchang Shouyi University, Wuhan 430064, Hubei, China;
[2]School of Engineering, Information Science Institute, Dalian Polytechnic University, Dalian 116033, Liaoning, China;
[3]Hubei Key Laboratory of Advanced Technology for Automotive Components, Wuhan University of Technology, Wuhan 430070, China;
[4]Hubei Collaborative Innovation Center for Automotive Components Technology, Wuhan University of Technology, Wuhan 430070, China;
[5]Hubei Research Center for New Energy & Intelligent Connected Vehicle, Wuhan University of Technology, Wuhan 430070, China;
[6]School of Computer and Information, Three Gorges University, Yichang 443002, Hubei, China.

Corresponding Author: Qing Li, Email: 2009111006@wsyu.edu.cn

Abstract: Aiming at the problem of fewer bands of Gaofen-1 satellite sensors, which makes it difficult to realize accurate cloud localization under the restriction of limited band information, an adaptive cloud detection method based on four bands is proposed. The method combines the physical properties of clouds, adopts the improved Haze Optimized Transform (HOT) index for the radiometrically calibrated Gaofen-1 remote sensing images, selects three sub-positional values of the histogram for threshold segmentation, and introduces the maximum interclass variance method based on this method, which takes the maximum variance value as the threshold of the average reflectance index for image segmentation, and combines the visible band ratio and the cloud in the blue wave with the cloud in the blue wave. Based on this method, the maximum inter-class variance method is introduced, and the maximum variance value is used as the threshold value of the average reflectance index for image segmentation, and at the same time, combining with the visible band ratio and the optical properties of the cloud in the blue band, the final cloud mask is obtained by multiple corrections through the cascade of multi-class indicators. The experimental results show that the proposed method makes the average accuracy of cloud recognition as high as 94.52% and the average precision rate as high as 98.97%, which improves the traditional threshold cloud detection accuracy and at the same time, it can be used to prepare labeled data to provide objective validation sets for remote sensing imagery in the process of exploring the field of deep learning.

Keywords: cloud detection; threshold segmentation; remote sensing imagery;GF-1

1.Introduction

Cloud detection of remote sensing images, as a precursor to atmospheric inversion, can lay a solid foundation for subsequent cloud culling, cloud classification and other meteorological applications [1], at this stage, cloud detection based on deep learning is the current mainstream means of cloud detection, but high-quality labeled data is a prerequisite for its high accuracy, and at present the ability to quickly and with a certain degree of accuracy of the dataset to provide deep learning algorithms to provide training for the training of the model. Training is still not well solved, for this reason, the design of simple and efficient cloud detection methods to make a pavement for the rapid production of cloud labeling data is the main content of this paper.

According to the data provided by the International Satellite Cloud Climatology Program (ISCCP), the average cloud coverage is about 67.5% globally, and the existence of clouds greatly restricts the accuracy of the atmospheric inversion in the corresponding subsurface region, so discriminating the existence of clouds and their

location information is an important element to improve the reliability of aerosol optical depth (AOD) inversion [2]. Among the existing cloud detection methods, among them, cloud detection relying on thresholding and spectral features, combined with regional image segmentation techniques are widely used due to their simple implementation, fast computation and stable performance. For example, Wang J et al [3] used cloud indices from a single PlanetScope satellite image with 3-meter resolution and reflectance anomalies in the image time series to generate an initial mask and then obtained the final mask through morphological processing.Chen et al [4] proposed a new method for cloud detection in Sentinel-2 images based on segmentation a priori and multiple features, which utilizes spectral, texture and exponential features to enhance the difference between clouds and the surface, while the segmentation results are used as a priori information to constrain the preclassification results, which improves the edge accuracy of cloud detection.Yongzheng Zhou et al [5] utilized an ultra-high resolution image and proposed bi-lateral texture filtering for cloud detection; due to the fact that clouds and snow possess higher brightness attributes, Xu et al [6] proposed to utilize a secondary detection strategy to improve the detection accuracy, while Dong et al [7] based on the radiative transfer model, performed targeted cloud detection on high brightness ice and snow subsurface in the polar region to solve the problem of cloud detection in a specific region.

In addition, there are many researchers using machine learning for cloud detection in recent years, based on the variety of cloud types, in order to add more validation information, Workman S [8] utilized multi-image fusion to guide single-image cloud detection, and by collecting a large Sentinel-2 image dataset as well as experimentally proving the semantic tagging of each pixel of land cover, the method reduces the label data dependency, and the cloud detection performance is improved; Min Xia et al [9] proposed a multi-scale fusion attention network to improve the accuracy and generality of cloud snow recognition based on the fact that the existing deep learning models could not get satisfactory results.J Yao et al [10] proposed a footprinting based on deep learning using a laser altimeter capable of acquiring high-precision long-distance three-dimensional coordinates on-board GF-7 satellite image cloud detection scheme; Li Zhang et al [11] proposed cloud detection with ACON and CAA-UNet by combining the attention mechanism on the basis of U-Net, obtaining higher overall accuracy of cloud detection on Landsat-8 and high-resolution coverage validation datasets.

Scholars at home and abroad on different types of remote sensing data, cloud detection based on traditional algorithms, mainly for specific categories of clouds to do accurate positioning; the use of spectral features to extract cloud areas; combined with cloud texture features for cloud positioning; according to multi-spectral characteristics to join a variety of infrared waves to synchronize identification of the cloud area; the use of optical satellite sensors and ground-based radar detection system, synchronous identification of corrected cloud areas; but the obvious shortcomings is that most of the traditional algorithms in the The segmentation threshold of most traditional algorithms relies on the a priori knowledge of researchers, and for multi-scene cloud detection, the high-precision identification relies on invisible spectral bands such as thermal infrared bands, which puts forward higher requirements for satellite-mounted sensors. Meanwhile, the multi-temporal phase detection method has problems such as strict data acquisition and the inability to avoid overlapping cloud areas.

Cloud detection based on the field of machine learning, the quality of remote sensing image dataset requirements are high, and the accuracy of cloud labeling data and the amount of data on the final results of the training model of the image is large, while the single view remote sensing images from a hundred kilometers of wide-format camera, the workload of manual labeling processing is extremely large, relying on the accumulation of knowledge and personal experience, and strong subjectivity. For this reason, the algorithm in this paper focuses on cloud detection accuracy and serves the work of remote sensing image labeling data generation, playing the classical threshold segmentation algorithm at the same time, combined with multi-index fine correction for cloud detection.

2. Materials and Methods

2.1 General data

The dataset of this thesis is selected from Gaofen-1 satellite WFV images [12], which is a publicly available dataset with calibrated L2 level data. It consists of 108 views of images on a global scale, covering the geography of different landscapes in different regions, mainly focusing on Asia, South America and North America.

2.3 Pretreatment work

The GF-1 data have four-band spectral information, namely, red, green, and blue bands and near-infrared bands, and different types of land surfaces in the images have the same kind of local similarity in the corresponding band pixel values, and the single-band statistical histograms usually have one or two wave peaks, and the bright white cloud pixel DN values are around 1023, and some of the image rendering effects are shown in Fig. 1. Since the bright surface is close to the cloud pixel value under clear sky conditions, it is easy to cause misdetection, for this reason, the HOT index is used to increase the difference between cloud and bright surface [13]. The specific formula is as follows:

$$HOT = （B_1 - \frac{B_3}{2}）(1 + \frac{B_1}{B_3+\epsilon}) \quad (1)$$

where B_1 and B_3 are the apparent reflectance of the blue and red bands, and ϵ is a small positive number that tends to zero.

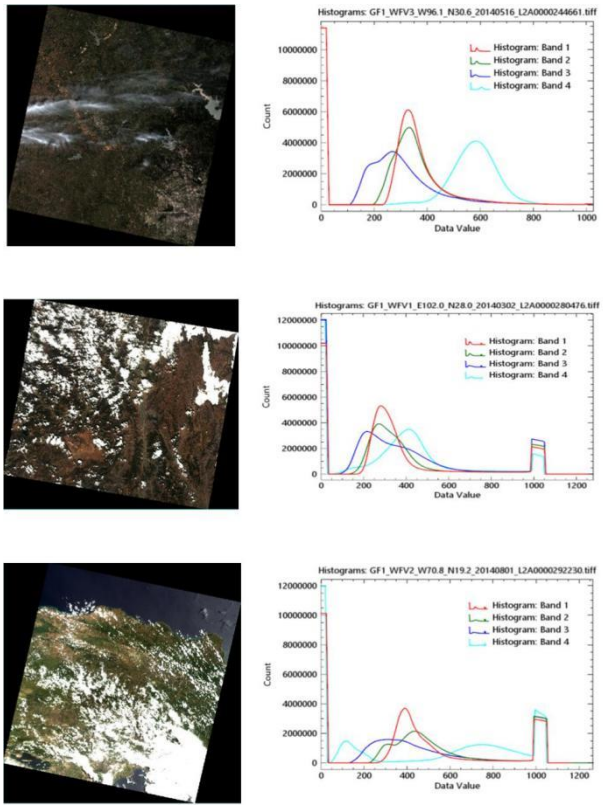

Fig. 1 Gray scale histogram of different images

From the HOT formula, it can be seen that for features with relatively high reflectance in the first band and low reflectance in the other bands, there are some limitations in distinguishing them from clouds, and it is considered that combining the Clound Index (CI) index and utilizing the optical properties of clouds that have high reflectance in all bands increases the variability of non-cloudy features that have low reflectance in all bands, so the average of the four bands of reflectance was taken and used to average the reflectance in all bands.

Due to the low transmittance of thick clouds, their reflectance in the blue, red and green bands is generally high, and the irradiance values of the cloud pixels in the image are close to each other, with the Visible Band Ratio (VBR) value close to 1. In order to effectively differentiate the cloud from the surface features, the normalized visible brightness ratio (NVBR) is used as a discriminant index. When the calculated VBR value in the remote sensing image exceeds the empirical threshold of 0.7, the pixel point can be categorized as a cloud pixel to improve the accuracy of cloud detection. The calculation formula of the optimized VBR is as follows:

$$VBR = \frac{B_1+B_2+B_3}{\max(B_1,B_2,B_3)+\epsilon}(1 + \frac{B_1B_2}{B_3+\delta}) \quad (2)$$

In the formula, B_1, B_2, and B_3 are the apparent reflectance of blue band, green band, and red band, respectively, ϵ and δ are as smaller positive numbers. Eq. further introduces a weight correction factor based on the traditional VBR calculation to enhance the differentiation between cloud pixels and highlighted surface features, thus improving the robustness of cloud detection.

2.3 Cloud mask extraction

Threshold segmentation is one of the commonly used means of cloud detection, in order to avoid the existence of the same image target region with a large luminance span leading to a single threshold segmentation of the cloud leakage detection, select the value at 70%, 80% and 90% of the three positions in the statistical histogram, respectively, set as the threshold T_1、T_2、T_3。The statistical gray frequency is stretched and transformed into a one-dimensional vector, and the HOT index is binarized according to the above thresholds to obtain three segmented images, and then the CI image is masked by the biplot to obtain the preliminary mask images P_1, P_2, P_3, respectively.Based on the Mistletoe optimized transformation index, a multilevel rough cloud mask is constructed, and the mask calculation can be obtained by the following discriminant: P_1, P_2, P_3:

$$M_i = \sigma(\alpha \cdot \left(\frac{HOT-T_i}{\beta+|HOT-T_i|}\right) + \gamma) \quad (3)$$

Where, M_i is the binarized image after masking, $\sigma(x)=\frac{1}{1+e^{-x}}$ is the Sigmoid function to make the segmentation result smoother and more stable, which can be taken as 1, 2, 3, hot is the Mistletoe Optimal Transformation Index,,α,$\beta$and $\gamma$are the tuning parameters, which are used for controlling the sensitivity of the cloud mask, the degree of thresholding smoothing, and the amount of offset, respectively. Here, the values are set to α=7,β=0.05 and γ=0.01, respectively.The traditional binarized cloud mask method uses hard threshold segmentation, but it may lead to misjudgment in the presence of fuzzy boundaries or highly reflective features (e.g., desert, snow). The above improved formulation introduces a smoothing factor through a nonlinear transformation, which makes the mask transition more naturally as the HOT approaches the threshold, thus reducing the effect of misclassification. In addition, the parameter α controls the segmentation sensitivity, which is set to a value of 7 here, β affects the degree of normalization of the HOT with respect to the threshold, which is set to a value of 0.05 here, and γ provides an overall offset adjustment to adapt to different observational conditions, and the value of γ is set to 0.01. in this paper. The method not only enhances the robustness of the cloud mask, but also can adapt to different remote sensing image scenes by adjusting the parameters to improve the applicability and accuracy of cloud detection.

On top of the previous step, the calculation of the maximum interclass variance of the cloud masks P_1, P_2, and P_3 is performed by M_i*CI The maximum value is found by traversing the method, and the masked CI image is stretched and processed so that the pixel values greater than the maximum interclass variance are equal to 1, and the rest are set to 0 to obtain the cloud and the subsurface region. The equation for calculating the interclass variance can be expressed as:

$$\sigma^2 = w_0 \cdot w_1 \cdot (\mu_0 - \mu_1) \cdot (\mu_1 - \mu_0) \quad (4)$$

Where, w_0, w_1 denote the ratio of the total number of pixels in the foreground region to the total number of pixels in the image, and the ratio of the total number of pixels in the background region to the total number of pixels in the image, respectively, and μ_0, μ_1 denote the respective average gray values of the foreground region and the background region, respectively, and then traverses the variance value and takes the maximum value as the optimal threshold value.

Since the reflectivity of clouds in remote sensing images has a certain regularity, with the help of the radiation value of the image in the experimental process, on the basis of determining the value of the thermal index and the visible band ratio parameter, dynamically change the different segmentation thresholds in the blue band, and the precision and accuracy of the resulting image cloud detection are shown in Fig. 2.

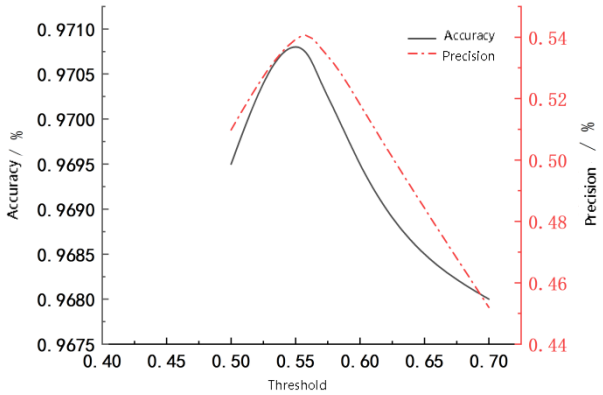

Fig. 2 Different threshold cloud detection results in blue band

When the reflectance of the blue band is greater than 0.56, the accuracy of cloud detection of the high-magnitude remote sensing image is the highest, and the precision rate is close to the highest value. In order to improve the precision rate of cloud detection, under the premise of satisfying the current conditions, the pixel unit that simultaneously meets the heat index HOT value greater than the OTSU value obtained after adaptive thresholding, as well as the visible-band-ratio VBR value greater than 0.7 is judged to be a cloud pixel, and the pixel value is set as 1, and those that do not satisfy the conditions are judged as non-cloud pixels and set to 0. The cloud detection results are finally obtained.

Results

Accuracy and Precision are commonly used as evaluation metrics in image classification, where Accuracy denotes the probability of predicting correctly in all samples, and Correctness denotes the probability that the prediction is a positive sample and it is actually a positive sample, with the expression:

$$\text{Accuracy} = \frac{TP + TN}{TP + TN + FP + FN} \tag{5}$$

$$\text{Precision} = \frac{TP}{TP + FP} \tag{6}$$

where TP denotes the number of positive samples judged as positive samples, TN denotes the number of positive samples judged as negative samples, FP denotes the number of negative samples judged as positive samples, and FN denotes the number of negative samples judged as negative samples. In this paper, all clouds are categorized as positive samples and the background is categorized as negative samples.

Figure 3 presents the effect of cloud detection using different thresholds and masking using the maximum inter-class variance achieved as the threshold, respectively:

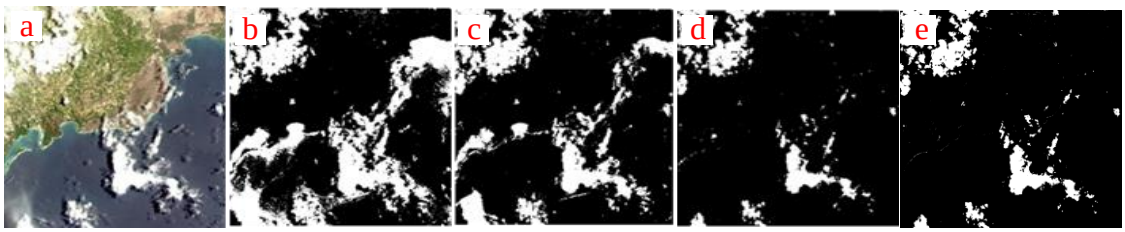

Fig. 3 Cloud segmentation renderings under different thresholds

（a is the original image, b, c and d are the segmentation results of threshold values T1, T2 and T3 respectively, and e is the result of cloud detection after correction）

As can be seen from Figure 3, when the threshold value is the 70% quantile of the statistical value of the grayscale histogram, the corresponding dichroic map has the largest number of cloud pixels and the largest cloud area, and there is obviously an over-extraction phenomenon, and at the expense of accuracy, the thin cloud area is extracted in a relatively complete manner; when the threshold value is the 80% quantile of the statistical value of the grayscale histogram, it abates the cloud area extracted from the 70% quantile, but there is still a wrong detection of the road and part of the water body with high albedo When the threshold value is 90% of the gray level histogram statistical value, it can correctly discriminate the waters in the image, can mask the bright roads, and the extraction of thick clouds is more accurate, and there are omissions in some thin clouds, and the accuracy rate of cloud detection is relatively good. Finally, the threshold segmentation is performed by the maximum interclass variance calculated after the three-threshold mask, and finally combined with the HOT index to calculate the specified thresholds for the blue band as well as the visible band ratio, which makes up for the lopsidedness of the single-threshold segmentation under the multilevel constraints and is able to shield the coasts, rivers, and roads in the image, and obtains the relatively complete cloud region, as in Fig. 3.

In order to further validate the effectiveness of the method, the accuracy and precision rates are tested on 108 view images respectively. Figure 4 demonstrates the corresponding accuracy and precision rates when the three-threshold segmentation is automatically selected according to each scene image during the adaptive threshold calculation process, and on this basis, Figure 5 shows the results of its accuracy and precision rates after fine correction by calculating its maximum OTSU as the final segmentation threshold.

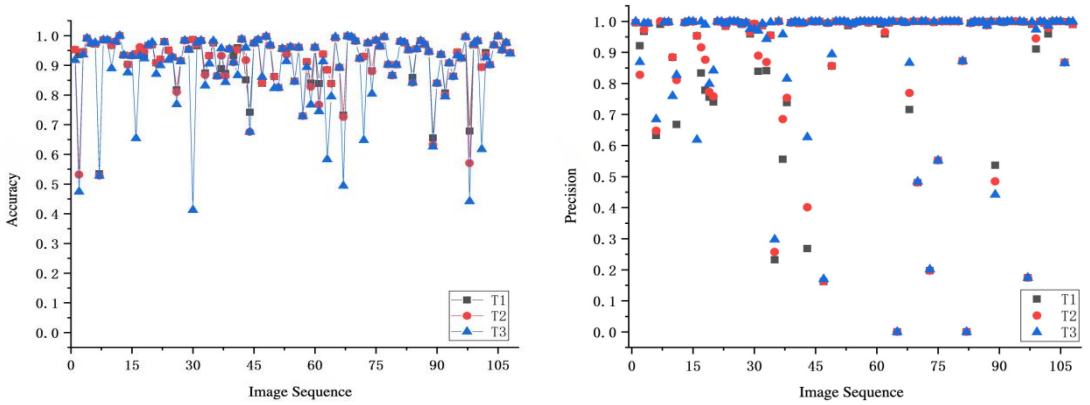

Fig. 4 Segmentation results with different thresholds

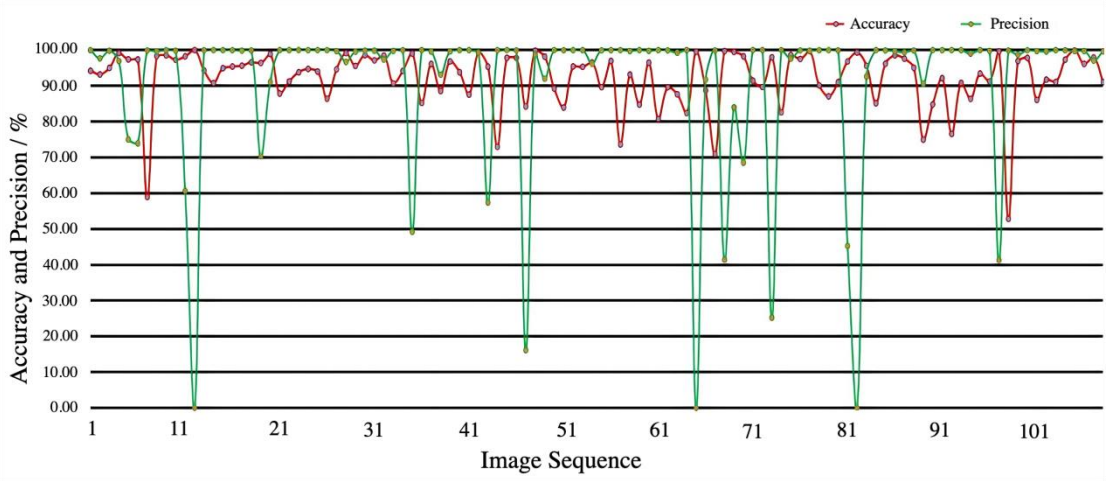

Fig. 5 Adaptive threshold cloud detection results

As can be seen from the analysis of Figure 5, after different thresholds for different surface discrimination, the adaptive cut-off point for 108 views of the data has a preliminary recognition accuracy, accuracy and precision rate has a regular distribution, most of the image cloud detection of the accuracy of more than ninety percent, the existence of about 7 views lower than 80%, while the accuracy rate is mostly close to 1, but there is a lower accuracy, the accuracy of the existence of the three views of the images of the three images corresponding to the 0 The numbering of the three images is:

1) GF1_WFV3_E146.8_S35.4_20131230_L2A0000356138.tiff;
2) GF1_WFV1_E24.0_S14.0_20130510_L2A0000017761.tiff;
3) GF1_WFV3_W97.0_N27.3_20140516_L2A0000244666.tiff

The observation of this three view image is found to be cloud free image. The percentage of cloud detection accuracy in different intervals is given in Fig. 6.

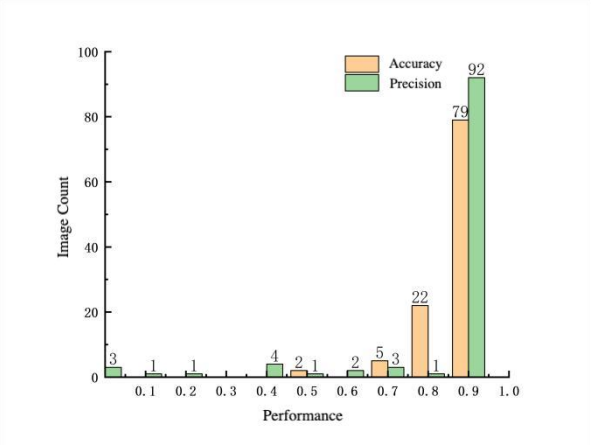

Fig. 6 Percentage of cloud detection accuracy for 108-scene imagery

As shown in Figure 6: there are 79 images with accuracy rate above 90%, of which 25 are between 90% and 95%, and 54 are between 95% and 99%, with an average accuracy rate of 92.31, and there are 16 images with accuracy rate lower than 90%, and the average accuracy rate of the remaining 92 images is 91.18%, of which 86 have an accuracy rate of 96% or above, and 76 have an accuracy rate of 99% or The average accuracy rate of the remaining 92 scenes is 91.18%, of which 86 scenes have an accuracy rate of 96% and 76 scenes have an accuracy rate of 99%.

Discussion

Under the qualitative evaluation index, the current algorithm is able to accurately recognize most of the clouds in the image, effectively excluding the easily mixed image elements of roads, coasts, and water bodies and other highlighted surfaces; under the quantitative evaluation index, excluding the cloud-free image and the low-cloud image, the average of the accuracy rate of cloud recognition is 94.52%, and the average of the precision rate is 98.97% in both cases, which is higher than that of the average accuracy rate of cloud detection in the literature [14] using the same data source for cloud detection with average accuracy. At the same time, at this stage, there are many scholars targeted cloud detection of specific remote sensing images, usually relying on the acquisition of multiple sources and according to the fusion to ensure the accuracy, and deep learning methods for model training of the amount of data and hardware equipment requirements, and based on the specificity of the data, it is not easy to quickly apply and migrate to the identification of other images, unless with the satellite has the same type of sensor construction and has similar additional information. This paper utilizes the GF-1 satellite, based on his only four-band data, with general remote sensing satellites have common characteristics, this paper's cloud detection method is simple and efficient, high detection accuracy, to meet the quantitative preparation of remote sensing labeling data needs.

It is worthwhile to note that the adaptive thresholding algorithm proposed in this paper is based on cloudy images and is not applicable to cloud-free images. Due to the existence of non-cloud features with highly similar

reflective properties to clouds in massive images, such as snow-covered areas, such pixels are very easy to be confused in the recognized cloud pixels, which greatly reduces the accuracy of the cloud detection of the algorithm proposed in this paper, and the introduction of other features in addition to spectral information such as geographic location information can be considered to exclude the identification of non-cloud pixels that are mixed up in the recognized cloud areas.

Conclusions

In this paper, for the limited band information high scores image data, combined with the physical characteristics of clouds, using the optimized HOT index, CI index, VBR, reflectance characteristics of blue band clouds, combined with adaptive OTSU to complete the task of cloud detection, to play the classical algorithms have the advantages of fast computing speed, low labor and time costs, in most cases can exclude the image of the high brightness of the body of water, and in the case of exclusion of less clouds or no cloud In the case of excluding little or no cloud, the cloud identification efficiency is high and applicable, solving the problem of less spectral information and difficult to locate the cloud pixels with high accuracy. The proposed new method is applicable to other optical satellite images with similar spectral settings, and can be used as a precursor to labeling the data in supervised classification methods.

Data sharing agreement

The datasets used and analyzed during the current study are available from the corresponding author on reasonable request.

Declaration of Conflicting Interests

The authors declared no potential conflicts of interest with respect to the research, author-ship, and publication of this article.

Funding

The authors received no financial support for the research.

References

[1] Yuan Zihao, Fu Guangliang, van Diedenhoven Bastiaan, Lin Hai Xiang, Erisman Jan Willem, Hasekamp Otto P. Cloud Masking for Multi-Angle Polarimetric Satellite Measurements Using a Neural Network Ensemble Approach[J]. Atmospheric Measurement Techniques, 2023, 16(10): 12345-12367.

[2] Wang F, Li Z, Jiang Q, Ren X, He H, Tang Y, Dong X, Sun Y, Dickerson RR. Comparative Analysis of Aerosol Vertical Characteristics over the North China Plain Based on Multi-Source Observation Data[J].. Remote Sensing. 2024; 16(4):609.

[3] Wang Jing, Yang Dedi, Chen Shuli, et al. Automatic cloud and cloud shadow detection in tropical areas for PlanetScope satellite images[J]. Remote Sensing of Environment, 2021, 264: 112604.

[4] Chen, Liangyu, Jun Pan, and Zhuoer Zhang. A Novel Cloud Detection Method Based on Segmentation Prior and Multiple Features for Sentinel-2 Images[J]. International Journal of Remote Sensing,2023, 44 (16): 5101–20.

[5] Zhou Yongzheng, Li Xu, Wei Baoguo, et al. A Bilateral Texture Filtering Based Cloud Detection Method for VHR Satellite Images[C]//2021 IEEE 16th Conference on Industrial Electronics and Applications (ICIEA), Chengdu, China, 2021: 1170-1175.

[6] XU Yun, XU Aiwen. Classification and detection of cloud, snow and fog in remote sensing images based on random forest[J]. Remote Sensing for Natural Resources, 2021, (1): 96-101.

[7] Dong S, Gong C, Hu Y, Zheng F, He Z. Polar Cloud Detection of FengYun-3D Medium Resolution Spectral Imager II Imagery Based on the Radiative Transfer Model. Remote Sensing. 2023; 15(21):5221.

[8] Scott Workman, M. Usman Rafique, Hunter Blanton, et al. Single Image Cloud Detection via Multi-Image Fusion[C]//IGARSS 2020 - 2020 IEEE International Geoscience and Remote Sensing Symposium, Waikoloa,

HI, USA,2020: 1468-1471.
[9] Min Xia, Yang Li, Yonghong Zhang, et al. Cloud/snow recognition of satellite cloud images based on multiscale fusion attention network[J]. Journal of Applied Remote Sensing, 2020, 14(3): 032609.
[10] Yao Jiaqi, Tang Xinming, Li Guoyuan, et al. Cloud detection of GF-7 satellite laser footprint image[J]. IET Image Processing, 2021, 15(10): 2127-2134.
[11] Zhang Li, Sun Jiahui, Yang Xubing, et al. Improving Deep Learning-Based Cloud Detection for Satellite Images with Attention Mechanism[J]. IEEE Geoscience and Remote Sensing Letters, 2022, 19:1-5.
[12] Li Zhiwei, Shen Huanfeng, Li Huifang, et al. Multi-feature combined cloud and cloud shadow detection in GaoFen-1 wide field of view imagery[J]. Remote sensing of environment, 2017, 191: 342-358.
[13] Zhang Ying, Guindon B, Cihlar Josef. An image transform to characterize and compensate for spatial variations in thin cloud contamination of Landsat images[J]. Remote Sensing of Environment, 2002, 82(2-3): 173-187.
[14] Hu C M，Zhang Z and Tang P. 2023. Research on multispectral satellite image cloud and cloud shadow detection algorithm of domestic satellite[J].National Remote Sensing Bulletin,2023,27(03):623-634.